Optimal pulse charging for the inhibition of curved dendrites

Asghar Aryanfar[a,*], Daniel J. Brooks[b], William A. Goddard[b]

[a] *Engineering faculty, Bahcesehir International University, Istanbul, Turkey 34349*
[b] *Engineering and Applied Science, California Institute of Technology, Pasadena, CA 91125*

Abstract

Lithium shows great promise as a material in high energy density batteries, however, lithium dendrites growth limits the safety and allowable operating condition for such devices. In this paper, we address the role of square wave pulse on the growth dynamics of curved dendrites on the continuum scale and large time periods by formulating analytical criteria. We quantify the optimum rest period based on the interplay between *diffusion* and *electromigration* as key factors for ionic flux. The accumulation of cations during pulse period in the vicinity of dendritic tips can relax during a subsequent rest period, preventing further local exponential deposition/growth. Our dimension-free analysis permits the application our results to a variety of electrochemical systems in diverse scales.

Keywords: Pulse charge, dendrites, concentration gradients

1. Introduction

Lithium metal is arguably one of the most promising anode candidate materials for use in high-energy and high-power density rechargeable batteries. [1] Possessing the lowest density and smallest ionic radius, lithium has a very high gravimetric energy density ($\rho = 0.53\ g.cm^{-3}$). Furthermore lithium is

*Corresponding author: aryanfar@caltech.edu

the most electropositive metal ($E^0 = -3.04V$ vs SHE), therefore coupling with any other cathode compound, it will likely provide the highest possible voltage, making it suitable for high-power applications such as electric vehicles.[2] The prominent issue with the lithium comes from its very low surface energy, leading to the formation of thermodynamically favorable branched dendrites during electrodeposition during each charge period.[3] The exponentially growing amorphous structures can occupy a large volume in the cell, possibly could reach the cathode and short the cell. Dendrites can also detach from their thinner necks through electrodissolution during subsequent discharge period. The amorphous growth of branched dendrites is general to all rechargeable batteries. Consequently, inhibition of dendrites is a major challenge for utilization of lithium in rechargeable batteries. Researchers have investigated how dendrites growth depends on such factors as current density, [4] electrode surface morphology[5, 6, 7, 8] and impurities [9, 10], solvent and electrolyte chemical composition [11, 12, 13], electrolyte concentration [14], powder electrodes [15], adhesive polymers[16], temperature [17, 18]and mechanics [19]. Recent conventional characterization techniques also include NMR [20] and MRI. [21]

Earlier model of dendrites had focused on the electric field and space charge as a responsible mechanism [22] while the later models focused on how ionic concentrations affect diffusion limited aggregation (DLA). [23] These mechanisms all relate to the electrochemical potential [24], indicating that each could be dominant, depending on the localizations of the electric potential or ionic concentration in the cell domain. However their interplay remains to be explored, especially in continuum and larger time periods.

Pulse method has been qualitatively proved as a powerful approach for den-

drite prevention [25], which has been utilized before for uniform electroplating.[26] Previously we found experimentally that the optimum rest period is related to the relaxation of double layer in the blocking electrode system [27] which can be expressed as RC time. [28] We explained qualitatively how relatively longer pulse periods with identical duty cycles (or idle ratio) will lead to longer exponentially growing dendrites. We developed coarse grained computationally affordable algorithm that allowed us to reach to the experimental time scale (ms), which provided insights for current study.

Dendrites instigation is rooted in the non-uniformity of electrode surface morphology at the atomic scale combined with Brownian ionic motion during electrodeposition. Any asperity in the surface provides a sharp electric field that attracts upcoming ions as a deposition sink. Indeed the closeness of a convex surface to upcoming ions is another contributing factor. In fact, the same mechanism is responsible for the further exponential growth of dendrites in any scale. During each pulse period the ions accumulate at the dendrites tips (unfavorable) due to high electric field in convex geometry and during each subsequent rest period the ions tend to diffuse away to other less concentrated regions (favorable). The relaxation of ionic concentration during the idle period provided a useful mechanism to achieve uniform deposition and growth. We should emphasize that we study the scales far larger than the double layer (or stern layer [29]) which is relatively small and comparable to the Debye length. In such thin reduction sites, the ionic concentration is depleted and concentration approaches zero [30]; In contrast, our continuum-level study covers much larger scale, extending to the cell domain.

In this paper, we develop analytical criteria for optimizing the optimal pulse

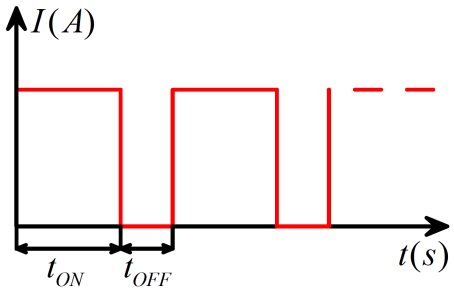

(a) Square pulse wave, illustrating the charge (t_{ON}) and idle (t_{OFF}) periods

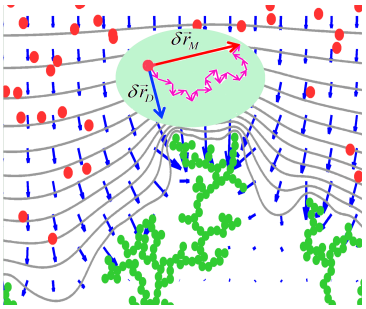

(b) Continuum-scale vectors: δr_D:diffusion length; δr_M: electromigration.

Figure 1: Schematics of **(a)** Pulse wave and **(b)** Ionic displacements during pulse period.

charging parameters. We perform dimensional analysis to set our formulation scale-free.

2. Methodology

In general, pulse charging in its simplest form consists of trains of square pulse wave (t_{ON}) and square rest (t_{OFF}) period of current (or voltage) (Fig. 1a). Therefore, it can uniquely be defined with two parameters. The *idle-ratio* (γ) determines how is the proportion of rest-to-charge period as:

$$\gamma = \frac{t_{OFF}}{t_{ON}} \tag{1}$$

while the *pulse frequency* (f) controls the repetition rate of pulse waves:

$$f = \frac{1}{t_{ON}} \tag{2}$$

Therefore the pulse duty cycle is simply: $D = \dfrac{1}{1+\gamma}$

In general the electrochemical flux is generated from the gradients of concentration (∇C) and electric potential ($\nabla \phi$). At the nanoscale, the ions of higher

concentration regions tend to collide and repel more and, given enough time, they diffuse to lower concentration regions following Brownian dynamics. In the continuum description, time scales larger than in inter-collision times scales (fs), these random movements can be described by the diffusion length ($\delta\vec{\mathbf{r}}_D$) as:

$$\delta\vec{\mathbf{r}}_D = \sqrt{2D^+\delta t}\hat{\mathbf{g}} \tag{3}$$

where $\vec{\mathbf{r}}_D$ is diffusion displacement of individual ion, D^+ is the cationic diffusion coefficient in the electrolyte,δt is the large time interval and $\hat{\mathbf{g}}$ is a random normal vector in space, representing Brownian dynamics. The diffusion length represents the average progress of a diffusive wave in a given time, which is obtained from diffusion equation. [31]

On the other hand, ions tend to acquire drift velocity in the electrolyte medium, given enough time, and their *electromigrative* progress is given as:

$$\delta\vec{\mathbf{r}}_M = \mu^+\vec{\mathbf{E}}\delta t \tag{4}$$

where $\delta\vec{\mathbf{r}}_M$ is the electromigration displacement, μ^+ is the mobility of cations in electrolyte, $\vec{\mathbf{E}}$ is the local electric field. Mobility is related to diffusivity by Einstein relation ($D = \mu RT$)[24] and electric field is gradient of electric potential ($\vec{\mathbf{E}} = -\nabla\phi$). Therefore the total effective displacement with neglecting convection ($Ra < 1500$) would be:

$$\delta\vec{\mathbf{r}} = \delta\vec{\mathbf{r}}_D + \delta\vec{\mathbf{r}}_M \tag{5}$$

The vector sum indicates the importance of directionality in Eqn. 5. The diffusion either can help the migration or can hurt it based on local gradients

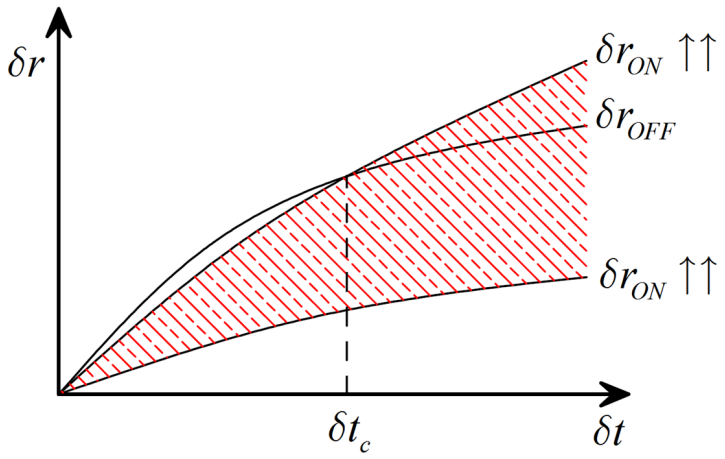

Figure 2: Time profile of progress range in pulse period, compared with diffusion lead during rest period. (Eqn. 7)

of concentration and electric potential. We split the characterization to find optimal idle ratio (section 2.1) and optimal rest period (section 2.2).

2.1. Optimum idle ratio (γ)

The ionic flux is the result of cumulative contribution from diffusion and electromigration. During pulse period both mechanisms are responsible for ionic flux, while the diffusion is the sole drive during the subsequent idle period for the relaxation. Therefore we base our formulation on the interplay between them. (Fig. 1b). Obviously, the diffusion length scales as $t^{\frac{1}{2}}$ and electromigration scales with t; Therefore comparing linear and square root trends, one expects that after giving a sufficient time δt_{eq} , the electromigration progress takes over the diffusion lead; the comparison leads to:

$$\delta t_{eq} = \frac{2RT}{\mu |\vec{\mathbf{E}}|^2} \tag{6}$$

The diffusion displacement is a random walk, therefore it can either contribute to electromigration or prevents its progress (Fig. 1b) , therefore for a

given fraction of time (δt), we have:

$$|\mu^{+}\vec{\mathbf{E}}\delta t| - |\sqrt{2D^{+}\delta t}| \leq |\delta\vec{\mathbf{r}}| \leq |\mu^{+}\vec{\mathbf{E}}\delta t| + |\sqrt{2D^{+}\delta t}| \tag{7}$$

where μ^{+}, $\vec{\mathbf{E}}$ and D^{+} are the local cations mobility, electric field and diffusivity respectively.

During each idle period, the concentrated ions in the dendritic tips tend to diffuse away. Therefore in order for destroy the concentration gradient created in the tip of dendrites during the charge, the average displacement during idle period has to be competitive enough (Fig.2) where:

$$|\sqrt{2D^{+}t_{OFF}}| \geq |\mu^{+}\vec{\mathbf{E}}t_{ON}| + |\sqrt{2D^{+}t_{ON}}| \tag{8}$$

without further look, it is obvious that $t_{OFF} > t_{ON}$, therefore $\gamma > 1$; further elaboration leads to:

$$\gamma - 2\sqrt{\gamma} + 1 - \frac{\mu^{+}|\vec{\mathbf{E}}|^{2}}{2RT}t_{ON} \geq 0 \tag{9}$$

which, considering $\sqrt{\gamma} \equiv x$ becomes a 2^{nd} order polynomial. The obtained solution δt_c would yield the minimum rest period for effective vanishment of the formed concentration gradients in the dendritic sights.(Fig. 4) The physically meaningful positive root for Eqn. 9 would be:

$$\gamma \geq \left(1 + \sqrt{\frac{\mu|\vec{\mathbf{E}}|^{2}t_{ON}}{2RT}}\right)^{2} \tag{10}$$

2.2. Optimum idle period

The steady state ionic concentration profile in the vicinity of curved electrodeposits can disappear during subsequent idle period, given sufficient time. The relaxation period of this concentration gradient doesnt necessarily need to

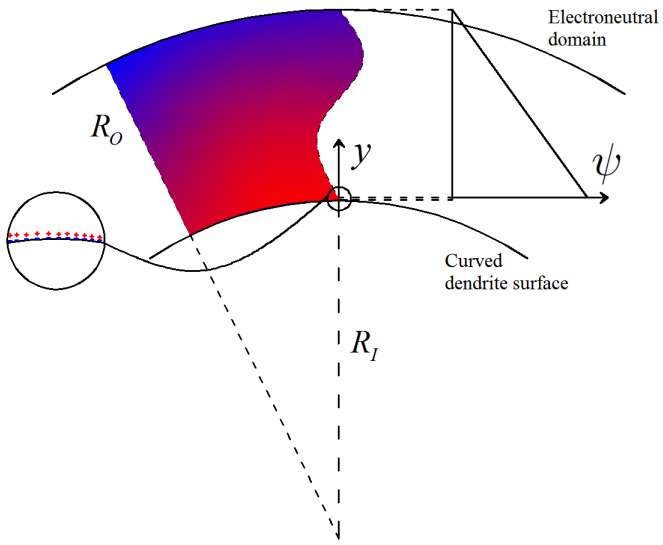

Figure 3: The curved dendrites with the concentration gradient the vicinity of surface.

be same as its establishment period (Sand's time [32]). It has been shown that the stern later (or electrical double layer) is in the order of Debye length and has magnitude of $\frac{D}{v}$ which is very small (D and v being the anionic diffusivity and deposit growth velocity).[33] Such relaxation for small scale diffuse double layer has been studied for flat blocking electrodes. [28] Herein, we address the relaxation in the continuum scale with curved boundary rising from the tip of growing dendrites.

Therefore from Fig. 3 we define dimensionless dendrite radial variable ξ as:

$$\xi = \frac{y}{R_O - R_I} \tag{11}$$

where R_I is the dendrite tip curvature and R_O is the radius of uniform concentration region, therefore $0 \leq \xi \leq 1$. Subsequently we can define the normalized concentration ψ as:

$$\psi = \frac{C(\xi) - C_0}{C_{max} - C_0} \tag{12}$$

where C_0 and C_{max} are the uniform and max concentrations respectively and $0 \leq \psi \leq 1$. The accumulation of ions occurs in this region where in continuum level possess radii of curvatures ranging from microns ($r \sim 10^{-6}$) to nearly flat surfaces ($r \to \infty$), therefore it is crucial to consider the curved geometry as a boundary. The simplified diffusion equation in polar 2D coordinates is:

$$\frac{\partial \psi}{\partial t} = D^+ \left(\frac{\partial^2 \psi}{\partial r^2} + \frac{1}{r} \frac{\partial \psi}{\partial r} \right) \tag{13}$$

which is invariant to the azimuthal direction for our purpose. In the inner surface (R_I) the flux (reduction rate) will be zero during rest period since there is no depletion. The dendrites would no accept any ions in this period. In the outer boundary (R_O) the concentration is identical to the rest of electroneutral medium which is in average constant, therefore:

$$\begin{cases} \dfrac{\partial \psi}{\partial y}(0, \xi) & = 0 \\ \psi(1, \xi) & = 1 \end{cases} \tag{14}$$

The other implication from this that the sum of total ions encapsulated in the region $\xi \in [0, 1]$ will be reduced in time:

$$\int_0^1 \psi(\xi, t) d\xi \leq \frac{1}{2} \tag{15}$$

2.3. Numerical solution

Eqn. 13 can be solved numerically by implementing finite difference scheme. Assuming ψ_i^j representing the normalized concentration in the normalized radial direction $\xi(i)$ at the time $t(j)$, discretization in the time (δt) and radial direction

(δr) gives:

$$\frac{\psi_i^{j+1} - \psi_i^j}{\delta t} = D^+ \left(\frac{\psi_{i+1}^j - 2\psi_i^j + \psi_{i-1}^j}{\delta r^2} + \frac{1}{r} \left(\frac{\psi_{i+1}^j - \psi_i^j}{\delta r} \right) \right) \tag{16}$$

which, considering dimensionless quotient $Q = \dfrac{D^+\delta}{\delta r^2}$, can be re-arranged for each individual finite-difference point as:

$$\psi_i^{j+1} = \left(1 - 2Q - \frac{\delta r}{r}Q\right) \psi_i^j + \left(Q + \frac{\delta r}{r}Q\right) \psi_{i+1}^j + Q\psi_{i-1}^j \tag{17}$$

Correspondingly the no-flux boundary conditions on the dendrite tip and the constant concentration on the outer boundary would translate in finite difference scheme into:

$$\begin{cases} \psi_1^j = \psi_2^j \\ \psi_{end}^j = 0 \end{cases} \tag{18}$$

Equation 17 should possess enough resolution in time (δt) to capture the variations in space (δr). Therefore the stability criterion for finite difference solution process requires:

$$1 - \frac{2D^+\delta t}{\delta r^2} - \frac{D^+\delta t}{r\delta r} \geq 0 \tag{19}$$

which in order to hold for $\xi \in [0, 1]$ will lead to:

$$\delta r \geq \frac{D^+\delta t}{2R_I} + \sqrt{\frac{D^{+2}\delta t^2}{4R_I^2} + 2D^+\delta t} \tag{20}$$

Considering this criterion, the Eqn. 13 can be solved numerically using finite difference method. The obtained profile generally has exponential decay behavior. In other words, as the concentration gradients becomes less, the rate of relaxation decreases as well, which vanishes for the concentration gradients,

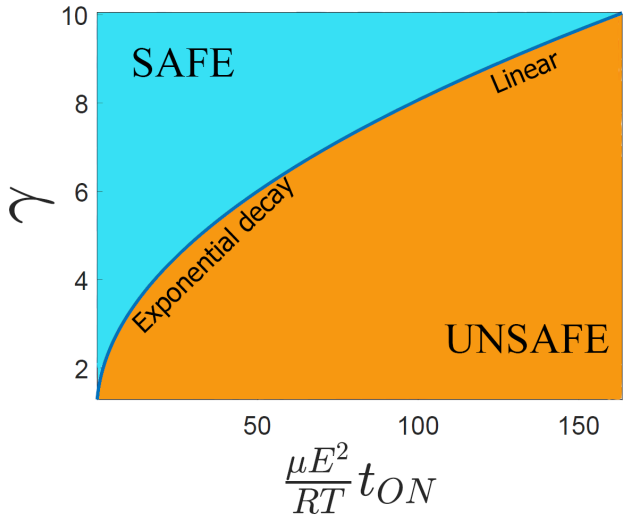

Figure 4: Behavior of idle ratio (γ) versus the dimension-less pulse period (t_{ON}), demonstrating initial exponential decay behavior, transiting gradually to linear regime.

very close to equilibrium. Further analysis would need significant time and computational power to pursue with no particular gain. Therefore we define the normalized relaxation error $\eta(t)$) as:

$$\eta(t) = \frac{\psi_{max}(t) - \psi_{min}(t)}{\psi_{0,max} - \psi_{0,min}} \tag{21}$$

which is a measure of how the concentration is close to the equilibrium.

3. Results and discussion

Eqn. 9 in fact represents the region in Fig. 2, where the possible solution lies within $\delta t \in [0, \delta t_c]$. This represents that the rest period lead to be competitive enough with average ionic progress in pulse period. Solving 2^{th} order polynomial, we obtain the relationship between idle ratio γ and the dimensionless value $\frac{\mu^+ \vec{\mathbf{E}}^2}{2RT} t_{ON}$. As stated previously, the ions diffuse w.r.t $\sim \sqrt{t}$ while they migrate as $\sim t$. Two regimes of behavior are obvious from Eqn. 9. Initially, the idle

ratio γ decays exponentially versus the dimension-less charge period t_{ON}. The exponential decay behavior indicates that relatively shorter amount of idle ratio is needed to catch up with the applied pulse period during relaxation. This is also obvious from Eqn. 9, as the term $\sqrt{\gamma}$ is comparable and in the order of γ. Later on for bigger values of t_{On}, the transition occurs and in the threshold the idle ratio becomes linearly proportional to dimension-free t_{ON}. In other words, with the increase of pulse period t_{ON} and neglecting the lower order offects, we reach the limit $\gamma \propto t_{ON}$, which directly means $t_{OFF} \propto t_{ON}^2$, therefore for higher applied pulse period t_{ON}, the equivalent idle period t_{OFF} for concentration relaxation has to be significantly higher. As well in the Eqn. 10 if t_{ON} increase indefinitely, the simplification will lead to linear relationship. Thus *fine-enough* pulse period is recommended for charge relaxation to be competitive with pulse effect. The general comparison of the pulse charging versus uniform charging of the same deposited ions remains an open question.

The relaxation dynamics in the curved geometry of dendritic deposits tip is shown in Fig. 5a. Having the identical ionic depth to relax into, the high curvature tips lead to more barrier for relaxation relative to flat surface. The underlying reason is the geometry of the domain. As the dendrite surface with smaller area and high concentration is exposed to expanded space on the outer radius ($R_O > R_I$) with lower concentration, there will be larger free domain to diffuse into, relative to flat surface. Therefore the relaxation occurs with lower speed for convex surfaces. This is also obvious from Eqn. 13 as the term $\frac{1}{r}\frac{\partial}{\partial r}$ becomes significant for higher curvatures and therefore would take more iterations to converge. Following the same phenomenology, the relaxation in concave surfaces occurs at faster rate relative to flat surface, as the concentrated atoms have relatively less space to diffuse into.

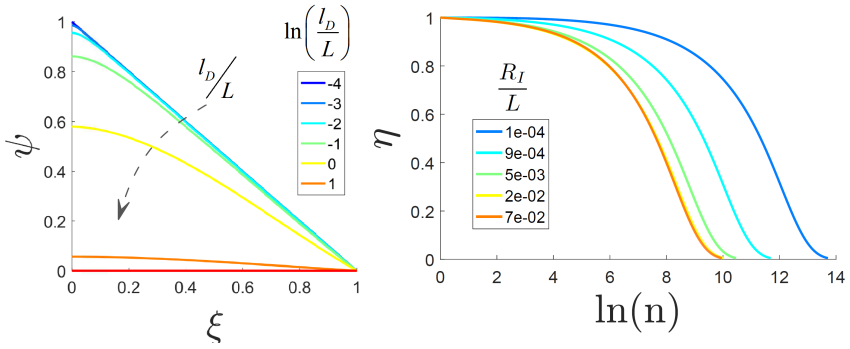

(a) Relaxation.

(b) Convergence.

Figure 5: **(a)** The relaxation of concentration gradient in time for $\frac{R_I}{L} = 10$ **(b)** The convergence of relaxation error (η) versus number of iterations (n) for various dimensionless dendrite tip radius ($\frac{R_I}{L}$).

4. Conclusions

In this paper, we have developed an analytical model for obtaining the most effective square pulse charging parameters for the given electrochemical cell based on the localizations of the ionic concentration and electric field. The dimensional analysis is performed to obtain the critical time threshold δt_c, which represents, the idle time period t_{OFF} required for the given corresponding pulse period t_{ON} is represented in terms of cell and solution transport properties. The nonlinear role of the dendrite curvature on the relaxation is demonstrated. The results are useful for estimating the optimum pulse role on the dendrite-prone electrochemical environment particularly those of involving lithium.

Acknowledgement

The authors would like to thank Prof. Martin Bazant (MIT) for the insightful comments on our earlier paper and Prof. Jaime Marian (UCLA) for help on analytical tools.

References

[1] Z. Li, J. Huang, B. Yann Liaw, V. Metzler, J. Zhang, A review of lithium deposition in lithium-ion and lithium metal secondary batteries, Journal of Power Sources 254 (2014) 168–182.

[2] W. Xu, J. Wang, F. Ding, X. Chen, E. Nasybulin, Y. Zhang, J.-G. Zhang, Lithium metal anodes for rechargeable batteries, Energy & Environmental Science 7 (2) (2014) 513–537.

[3] K. Xu, Nonaqueous liquid electrolytes for lithium-based rechargeable batteries, Chemical Reviews-Columbus 104 (10) (2004) 4303–4418.

[4] B. B. J. T. M. T. N. L. E. B. P. N. F. Orsini, A.D. Pasquier, In situ scanning electron microscopy (sem) observation of interfaces with plastic lithium batteries, Journal of power sources 76 (1998) 19–29.

[5] X. H. Liu, L. Zhong, L. Q. Zhang, A. Kushima, S. X. Mao, J. Li, Z. Z. Ye, J. P. Sullivan, J. Y. Huang, Lithium fiber growth on the anode in a nanowire lithium ion battery during charging, Applied Physics Letters 98 (18) 183107.

[6] C. Monroe, J. Newman, The effect of interfacial deformation on electrodeposition kinetics, Journal of the Electrochemical Society 151 (6) (2004) A880–A886.

[7] T. Nishida, K. Nishikawa, M. Rosso, Y. Fukunaka, Optical observation of li dendrite growth in ionic liquid, Electrochimica Acta 100 (2013) 333–341.

[8] C. P. Nielsen, H. Bruus, Morphological instability during steady electrodeposition at overlimiting currents, arXiv preprint arXiv:1505.07571.

[9] K. J. Harry, D. T. Hallinan, D. Y. Parkinson, A. A. MacDowell, N. P. Balsara, Detection of subsurface structures underneath dendrites formed on cycled lithium metal electrodes, Nature materials 13 (1) (2014) 69–73.

[10] J. Steiger, D. Kramer, R. Monig, Mechanisms of dendritic growth investigated by in situ light microscopy during electrodeposition and dissolution of lithium, Journal of Power Sources 261 (2014) 112–119.

[11] N. Schweikert, A. Hofmann, M. Schulz, M. Scheuermann, S. T. Boles, T. Hanemann, H. Hahn, S. Indris, Suppressed lithium dendrite growth in lithium batteries using ionic liquid electrolytes: Investigation by electrochemical impedance spectroscopy, scanning electron microscopy, and in situ li-7 nuclear magnetic resonance spectroscopy, Journal of Power Sources 228 (2013) 237–243.

[12] R. Younesi, G. M. Veith, P. Johansson, K. Edstrm, T. Vegge, Lithium salts for advanced lithium batteries: Li-metal, li-o 2, and li-s, Energy and Environmental Science 8 (7) (2015) 1905–1922.

[13] R. Khurana, J. Schaefer, L. A. Archer, G. W. Coates, Suppression of lithium dendrite growth using cross-linked polyethylene/polyethylene oxide electrolytes: A new approach for practical lithium-metal polymer batteries, Journal of the American Chemical Society.

[14] C. Brissot, M. Rosso, J. N. Chazalviel, S. Lascaud, Dendritic growth mechanisms in lithium/polymer cells, Journal of Power Sources 81 (1999) 925–929.

[15] I. W. Seong, C. H. Hong, B. K. Kim, W. Y. Yoon, The effects of current density and amount of discharge on dendrite formation in the lithium powder anode electrode, Journal of Power Sources 178 (2) (2008) 769–773.

[16] G. Stone, S. Mullin, A. Teran, D. Hallinan, A. Minor, A. Hexemer, N. Balsara, Resolution of the modulus versus adhesion dilemma in solid polymer electrolytes for rechargeable lithium metal batteries, Journal of The Electrochemical Society 159 (3) (2012) A222–A227.

[17] A. Aryanfar, D. J. Brooks, A. J. Colussi, B. V. Merinov, W. A. Goddard III, M. R. Hoffmann, Thermal relaxation of lithium dendrites, Physical Chemistry Chemical Physics 17 (12) (2015) 8000–8005.

[18] A. Aryanfar, T. Cheng, A. J. Colussi, B. V. Merinov, W. A. Goddard III, M. R. Hoffmann, Annealing kinetics of electrodeposited lithium dendrites, The Journal of chemical physics 143 (13) (2015) 134701.

[19] C. Xu, Z. Ahmad, A. Aryanfar, V. Viswanathan, J. R. Greer, Enhanced strength and temperature dependence of mechanical properties of li at small scales and its implications for li metal anodes, Proceedings of the National Academy of Sciences 114 (1) (2017) 57–61.

[20] R. Bhattacharyya, B. Key, H. L. Chen, A. S. Best, A. F. Hollenkamp, C. P. Grey, In situ nmr observation of the formation of metallic lithium microstructures in lithium batteries, Nature Materials 9 (6) (2010) 504–510.

[21] S. Chandrashekar, N. M. Trease, H. J. Chang, L.-S. Du, C. P. Grey, A. Jerschow, 7li mri of li batteries reveals location of microstructural lithium, Nature Materials 11 (4) (2012) 311–315.

[22] J. N. Chazalviel, Electrochemical aspects of the generation of ramified metallic electrodeposits, Physical Review A 42 (12) 7355–7367.

[23] C. Monroe, J. Newman, Dendrite growth in lithium/polymer systems - a

propagation model for liquid electrolytes under galvanostatic conditions, Journal of the Electrochemical Society 150 (10) (2003) A1377–A1384.

[24] A. J. Bard, L. R. Faulkner, Electrochemical methods: fundamentals and applications. 2 New York: Wiley, 1980.

[25] J. Li, E. Murphy, J. Winnick, P. A. Kohl, The effects of pulse charging on cycling characteristics of commercial lithium-ion batteries, Journal of power sources 102 (1) (2001) 302–309.

[26] M. S. Chandrasekar, M. Pushpavanam, Pulse and pulse reverse plating - conceptual, advantages and applications, Electrochimica Acta 53 (8) (2008) 3313–3322.

[27] A. Aryanfar, D. Brooks, B. V. Merinov, W. A. Goddard III, A. J. Colussi, M. R. Hoffmann, Dynamics of lithium dendrite growth and inhibition: pulse charging experiments and monte carlo calculations, The journal of physical chemistry letters 5 (10) (2014) 1721–1726.

[28] M. Z. Bazant, K. Thornton, A. Ajdari, Diffuse-charge dynamics in electrochemical systems, Physical Review E 70 (2).

[29] M. Z. Bazant, B. D. Storey, A. A. Kornyshev, Double layer in ionic liquids: Overscreening versus crowding, Physical Review Letters 106 (4) (2011) 046102.

[30] V. Fleury, Branched fractal patterns in non-equilibrium electrochemical deposition from oscillatory nucleation and growth, Nature 390 (6656) (1997) 145–148.

[31] R. B. Bird, W. E. Stewart, E. N. Lightfoot, Transport phenomena, John Wiley & Sons, 2007.

[32] M. Rosso, Electrodeposition from a binary electrolyte: new developments and applications, Electrochimica Acta 53 (1) (2007) 250–256.

[33] C. Leger, F. Argoul, M. Z. Bazant, Front dynamics during diffusion-limited corrosion of ramified electrodeposits, Journal of Physical Chemistry B 103 (28) (1999) 5841–5851.